Optics Communications 284 (2011) 1569–1574

Contents lists available at ScienceDirect

Optics Communications

journal homepage: www.elsevier.com/locate/optcom

Coherently induced double photonic band gaps in a driven N-type atomic system

Ren-Gang Wan [a], Jun Kou [a], Li Jiang [a], Shang-Qi Kuang [a,b], Yun Jiang [a], Jin-Yue Gao [a,*]

[a] Key Lab of Coherent Light and Atomic and Molecular Spectroscopy of Ministry of Education, College of Physics, Jilin University, Changchun 130023, China
[b] Changchun Institute of Optics, Fine Mechanics and Physics, Chinese Academy of Sciences, Changchun 130033, China

ARTICLE INFO

Article history:
Received 12 October 2010
Accepted 20 November 2010

ABSTRACT

In an N-type atomic system with double electromagnetically induced transparency, when the traveling-wave coupling field is replaced by a standing-wave, double fully developed photonic band gaps open up due to space-modulated refractive index within the two electromagnetically induced transparency widows. The dynamically induced band gaps can be tuned coherently, and have applications in manipulating the propagation dynamics of light pulses.

1. Introduction

The manipulation of light via quantum coherence and interference effects in optical medium interacting with laser fields has attracted extensive attention. Many fascinating phenomena have been revealed and studied in fundamentals and applications. One of the most typical schemes is the electromagnetically induced transparency (EIT) [1,2], which refers to an opaque medium on probe resonance that is made highly transparent by a coupling field. With the help of the EIT technique, one can well control the interaction between light and matter. Generally, a traveling-wave (TW) coupling field is adopted in the schemes of slow light [3], optical storage [4], enhancement of nonlinearity [5], etc. Yet, when the same three-level atom is driven by a standing-wave (SW), the optical response of the probe is modulated periodically in the space. When the weak probe field propagates perpendicularly to the standing-wave, the atomic medium acts as an electromagnetically induced grating and diffracts the probe into high-order diffractions [6]. If the propagation of the probe is along the standing-wave, the probe can be completely reflected, which has been explored to generate stationary light pulse [7–10], to achieve tunable photonic band gap [11–15], to devise a dynamic controlled cavity [16], to implement optical routing [17], etc.

For more practical applications, double photonic band gaps (PBGs) have been studied most recently. Using the spontaneously generated coherence (SGC) effect, Gao et al. obtained double PBGs in a four-level system [18]. Cui et al. proposed a scheme to achieve double PBGs in a tripod configuration driven by two SW fields [19]. Kuang et al. attained double PBGs in N-type atoms utilizing spatial dependent double-dark resonances induced by an SW control field [20]. In a microwave driven generic four-level atoms, we also get well performed double PBGs [21]. However, it is very difficult to find a system exhibiting SGC in real atoms, two SW and microwave increase the complexity in the experiment. Moreover, though an N-scheme is easy to realize, the transparency positions change in the space, therefore, the probe field undergoes absorption and one cannot get well performed double PBGs with high reflectivity [20].

In this paper, we demonstrate a scheme for double PBGs in an N-type system driven by an SW coupling field. In the previous N-type system [11,20], a standing-wave is utilized to couple the Λ-EIT to another level. When the standing-wave is off resonant with large detuning, one can obtain enhanced space-dependent nonlinear refractivity accompanied by vanishing absorption for the probe, hence one PBG with high transmissivity occurs around the EIT point [11]. While the standing-wave is resonant, the refractivity is modulated in the space as well as the probe absorption, the resulting double-dark resonances, i.e. the double transparency positions, are changed in the space and then reduce the reflectivity of the double PBGs [20]. However, in the present scheme, the standing-wave serves as the coupling field for EIT, and a traveling-wave is used to split the single dark resonance into double ones. The transparency positions here are kept fixed and the refractive index is spatial modulated in the two EIT windows. Therefore, double PBGs open up in the two EIT regions with higher reflectivity than that in Ref. [20]. The double PBGs are controllable and allow us simultaneously to manipulate the propagation of two light pulses.

2. Model and equations

Considering a four-level N-type atomic system shown in Fig. 1, the exited state $|3\rangle$ is coupled to the ground states $|1\rangle$ and $|2\rangle$ by a strong SW coupling field with spatial dependent Rabi frequency $\Omega_c(x)$ and a weak probe field Ω_p, respectively. Therefore, a conventional Λ-type EIT configuration is formed. However, the resulting single dark state is coupled to another state $|4\rangle$ by a control field Ω_d, and hence double-dark resonances arise as a result of a coherent interaction.

* Corresponding author.
E-mail address: jygao@mail.jlu.edu.cn (J.-Y. Gao).

0030-4018/$ – see front matter © 2010 Elsevier B.V. All rights reserved.
doi:10.1016/j.optcom.2010.11.060

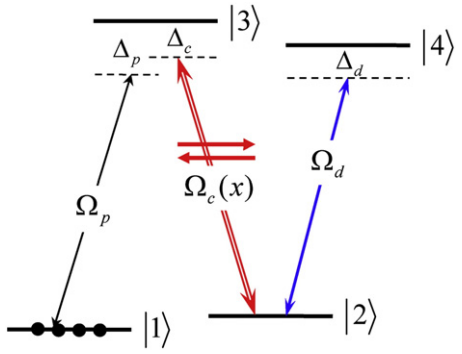

Fig. 1. Schematic diagram of a four-level N-type atomic system. A weak probe field Ω_p and a strong standing-wave coupling field $\Omega_c(x)$ couple the transitions $|1\rangle \leftrightarrow |3\rangle$ and $|2\rangle \leftrightarrow |3\rangle$, respectively, while the transition $|2\rangle \leftrightarrow |4\rangle$ is driven by a control field Ω_d.

To deal with the properties of such an SW driven system, we start with its steady optical response. In the limit of a weak field, we can analytically solve the Liouville equation in the steady state and derive the off-diagonal density matrix element:

$$\rho_{31} = \frac{\Omega_p\left(\gamma'_{21}\gamma'_{41}-\Omega_d^2\right)}{\gamma'_{31}\left(\gamma'_{21}\gamma'_{41}-\Omega_d^2\right)-\gamma'_{41}\Omega_c^2(x),} \tag{1}$$

where $\gamma'_{21}=\Delta_p-\Delta_c-i\gamma_{21}$, $\gamma'_{31}=\Delta_p-i\gamma_{31}$, and $\gamma'_{41}=\Delta_p-\Delta_c+\Delta_d-i\gamma_{41}$, with γ_{i1} $(i=2,3,4)$ being the decoherence rate of the respective atomic coherence ρ_{i1}, and $\Delta_p=\omega_{21}-\omega_p$, $\Delta_c=\omega_{23}-\omega_c$, and $\Delta_d=\omega_{42}-\omega_d$ are detunings of the three fields from the corresponding transitions.

Unlike in typical double-dark resonances system where a TW coupling field is applied, the coupling here is in the SW pattern as generated from the retroreflection on a mirror of reflectivity R_m. Then the resulting squared coupling Rabi frequency, which varies periodically along the x axis, can be written as

$$\Omega_c^2(x) = \Omega_0^2\left[\left(1+\sqrt{R_m}\right)^2 cos^2(k_c x) + \left(1-\sqrt{R_m}\right)^2 sin^2(k_c x)\right], \tag{2}$$

where k_c denotes the wave vector of the coupling field. It is obvious that $\Omega_c^2(x)$ has a spatial periodicity of $a=\lambda_c/2$, which may be changed into $a=\lambda_c/[2\cos(\theta/2)]$ via slightly misaligning the forward and backward coupling fields by an angle θ.

The periodical Rabi frequency induces space-dependent linear susceptibility χ_p and refractive index n_p for the probe, which are given by

$$\chi_p\left(\Delta_p,x\right) = 3\pi\mathcal{N}\frac{\gamma_{31}\left(\gamma'_{21}\gamma'_{41}-\Omega_d^2\right)}{\gamma'_{31}\left(\gamma'_{21}\gamma'_{41}-\Omega_d^2\right)-\gamma'_{41}\Omega_c^2(x),} \tag{3}$$

$$n_p\left(\Delta_p,x\right) = \sqrt{1+\chi_p\left(\Delta_p,x\right)}, \tag{4}$$

where $\mathcal{N}=N_0\left(\lambda_p/2\pi\right)^3$, N_0 is the atomic density. With the complex refractivity $n_p(\Delta_p,x)$ in hand, we further obtain the 2×2 unimodular transfer matrix $M(\Delta_p)$ describing the probe propagation through a single period of length a. Then, the translational invariance of the periodic medium is fulfilled by imposing the Bloch condition on the photonic eigenstates, i.e.

$$\begin{pmatrix}E^+(x+a)\\E^-(x+a)\end{pmatrix} = M\left(\Delta_p\right)\begin{pmatrix}E^+(x)\\E^-(x)\end{pmatrix} = \begin{pmatrix}e^{i\kappa a}E^+(x)\\e^{i\kappa a}E^-(x)\end{pmatrix}, \tag{5}$$

where E^+ and E^- denote the amplitudes of the forward and backward electric fields of the probe, respectively. $\kappa=\kappa'+i\kappa''$ is the complex Bloch wave vector, which represents the PBG structure, and can be derived from the solutions of equation $e^{2i\kappa a}-\mathrm{Tr}[M(\Delta_p)]e^{i\kappa a}+1=0$ with $\det M=1$ [13]. Noting that both κ and $-\kappa$ are the solutions of the equation, one obtains

$$\kappa a = \pm\, cos^{-1}\left[\frac{\mathrm{Tr}\left[M\left(\Delta_p\right)\right]}{2}\right]. \tag{6}$$

The Bloch wave vector describes the photonic band structure for a probe in infinite periods. Yet we concentrate on the propagation through a sample of finite length. For a sample of length $l=Na$ with N being the number of the SW periods, the total transfer matrix can be expressed as $M_N=M^N$, and the reflection and transmission amplitudes for the probe are given by

$$\begin{aligned} r(\Delta_P) &= \frac{M_{N(12)}(\Delta_P)}{M_{N(22)}(\Delta_P)} = \frac{M_{12}\,sin(N\kappa a)}{M_{22}\,sin(N\kappa a)-sin[(N-1)\kappa a]},\\ t(\Delta_P) &= \frac{1}{M_{N(22)}(\Delta_P)} = \frac{sin(\kappa a)}{M_{22}\,sin(N\kappa a)-sin[(N-1)\kappa a]}, \end{aligned} \tag{7}$$

with $M_{N(ij)}$ being the matrix elements of M_N. Then we can easily obtain the reflectivity $R(\Delta_P)=|r(\Delta_P)|^2$ and the transmissivity $T(\Delta_P)=|t(\Delta_P)|^2$.

By utilizing Eq. (7) and the Fourier transform method [15], one can study the propagation dynamics of an incident probe pulse. Here, we assume that the input probe has Gaussian profiles in the time and frequency domains as

$$\begin{aligned} E_{It}(t) &= E_{0t}e^{-(t-t_0)^2/\delta_t^2},\\ E_{If}\left(\Delta_p\right) &= E_{0f}e^{-\left(\Delta_p-\Delta_{p0}\right)^2/\delta_p^2}, \end{aligned} \tag{8}$$

where $E_{0f}=\sqrt{\pi}\delta_t E_{0t}$, $\delta_p=2/\delta_t$, t_0 and δ_t (Δ_{p0} and δ_p) denote the center and width of the input probe pulse in the time (frequency) domain.

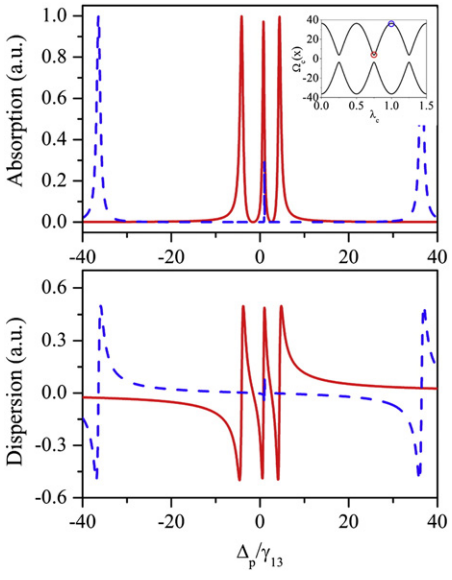

Fig. 2. The probe absorption and dispersion at the nodes (red—solid) and antinodes (blue—dashed) of the standing-wave. Parameters are $\gamma_{21}=1.0$ kHz, $\gamma_{31}=14.0$ MHz, $\gamma_{41}=91.0$ kHz, $\Omega_0=20\gamma_{31}$, $\Omega_d=2\gamma_{31}$, $\Delta_c=0$, $\Delta_d=-1\gamma_{31}$, $\eta=0.1$, $\theta=18$ mrad.

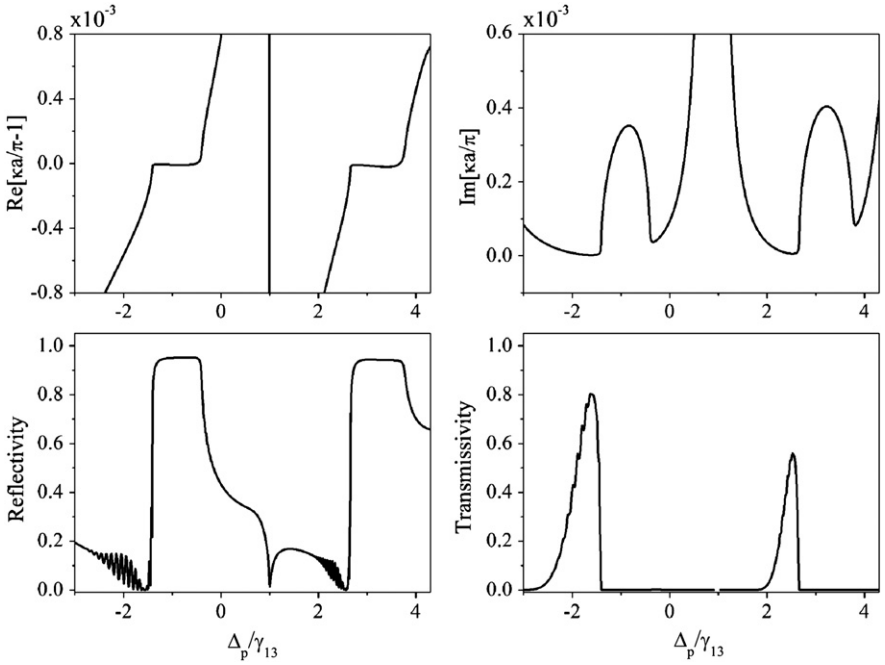

Fig. 3. Photonic band gap structure near the first Brillouin zone boundary in terms of the Bloch wave vector, and the probe reflectivity and transmissivity spectra for a 1.0 cm long sample (atomic density is $N=1.0\times10^{12}\,\mathrm{cm}^{-3}$). Other parameters are the same as in Fig. 2.

Then the reflected and the transmitted Fourier components can be derived from $E_{Rf}(\Delta_p)=E_{If}(\Delta_p)\cdot r(\Delta_p)$ and $E_{Tf}(\Delta_p)=E_{If}(\Delta_p)\cdot t(\Delta_p)$, so that we obtain the reflected and transmitted probe pulse in the time domain via inverse Fourier transform given by

$$E_{Rt}(t)=\int E_{Rf}\left(\Delta_p\right)e^{i(\Delta_p-\Delta_{p0})t}d\left(\Delta_p\right),\qquad E_{Tt}(t)=\int E_{Tf}\left(\Delta_p\right)e^{i(\Delta_p-\Delta_{p0})t}d\left(\Delta_p\right). \tag{9}$$

3. Results and discussions

3.1. Double PBGs

As shown by Lukin et al. [22], in a generic four-level system the coherent perturbation leads to the splitting of the single dark state and the emergency of double-dark resonances, which indicates a pair of EIT windows for the probe field. Generally, this effect is induced by a microwave driving a magnetic dipole transition or by optical fields driving a two-photon transition in order to get a neglectable decoherence rate for perfect double-dark resonances or complete transparency. However, the probability of a magnetic dipole transition or a two-photon transition is very small, hence it restricts the manipulation of the double-dark resonances. Here we consider the ^{171}Yb (I=1/2) cold atoms [23], where the states $|1\rangle$, $|2\rangle$, $|3\rangle$ and $|4\rangle$ respectively correspond to $|^1S_0,F=1/2,m_F=-1/2\rangle$, $|^1S_0,F=1/2,m_F=1/2\rangle$, $|^1P_1,F=1/2,m_F=-1/2\rangle$ and $|^3P_1,F=1/2,m_F=1/2\rangle$. The decoherence rates are $\gamma_{31}=\Gamma_3/2=14.0$ MHz and $\gamma_{41}=\Gamma_4/2=91.0$ kHz. Clearly, $|2\rangle\leftrightarrow|4\rangle$ is one-photon transition and $\gamma_{41}\ll\gamma_{31}$. Therefore, the control field Ω_d can lead to a pair of EIT windows with a complete transparency at the two frequencies $\Delta_\pm=\left(2\Delta_c-\Delta_d\pm\sqrt{\Delta_d^2+4\Omega_d^2}\right)/2$, which can be derived from the vanishing probe susceptibility of Eq. (3). In the present scheme, as a result of the SW coupling field, the probe absorption and dispersion are modified spatially along the x axis with the same periodicity as the SW. It is worth mentioning that an imperfect SW coupling with unequal forward and backward components is applied so that double EIT windows are established everywhere, even at the nodes of the SW (see Fig. 2). We here define a parameter $\eta=(1-\sqrt{R_m})/(1+\sqrt{R_m})$ to describe the degree of imperfectness of the SW. As can be seen in Fig. 2, the nodes of the SW correspond to the narrow EIT windows with a steep dispersion, while the antinodes correspond to the wide EIT windows with a flat dispersion. Therefore, the probe field propagates as in a one-dimensional multilayer periodic structure which has two transparent regions. Consequently double PBGs are expected to occur at the Brillouin zone boundary π/a.

The resulting PBGs structure is shown in terms of the Bloch wave vector and the reflection and transmission spectra (see Fig. 3). We obtain a pair of PBGs which opened up in the frequency ranges where $\kappa'=\pi/a$ and $\kappa''\neq0$. Within the gaps, $\kappa''\neq0$ corresponds to the reflection rather than the absorption and the probe reflectivity is over 95%. The left edges of the double PBGs, where the reflectivity is zero,

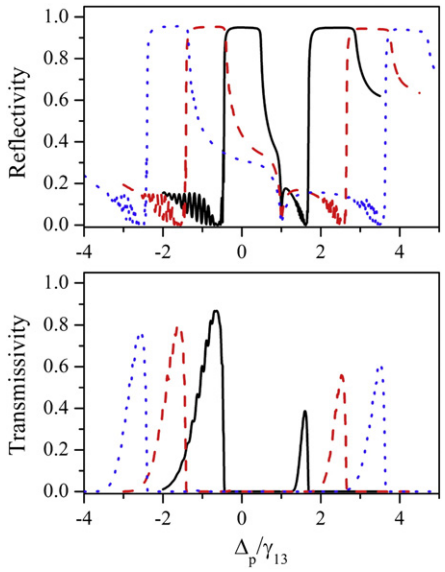

Fig. 4. Photonic band gap structure for different control intensities with $\Omega_d=1.0\gamma_{31}$ (black solid), $\Omega_d=2.0\gamma_{31}$ (red dashed), and $\Omega_d=3.0\gamma_{31}$ (blue dotted). Other parameters are the same as in Fig. 2.

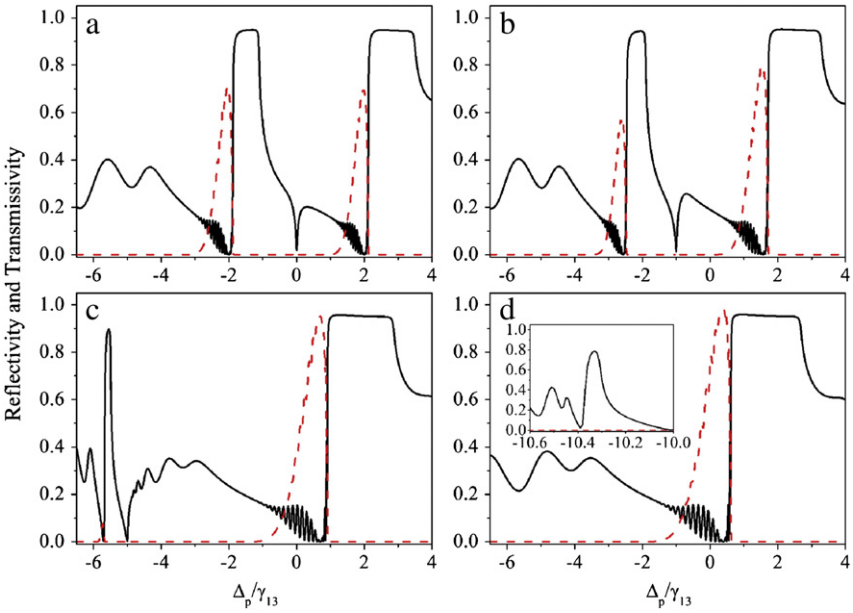

Fig. 5. Photonic band gap structure for different positive control detunings, (a) $\Delta_d=0$, (b) $\Delta_d=1.0\gamma_{31}$, (c) $\Delta_d=5.0\gamma_{31}$, and (d) $\Delta_d=10.0\gamma_{31}$. Other parameters are the same as in Fig. 2. The black solid line and red dashed line correspond to the reflectivity and transmissivity, respectively.

are determined by the two dark resonances which occur at $\Delta_\pm = \left(2\Delta_c - \Delta_d \pm \sqrt{\Delta_d^2 + 4\Omega_d^2}\right)/2$. Beside the left band edges, there are two narrow transmission regions of the probe. Due to $\Delta_d=-1$, the right EIT window in the nodes of the SW is narrower than the left as a result of the interacting double-dark resonances as shown in Fig. 2. Thus the more absorption and the less transmission are in the right transmission region.

3.2. Tunable double PBGs

One of the significant characters of the dynamically induced double PBGs is the tunability. As referred in the previous discussion, the left band edges depend on $\Delta_\pm = \left(2\Delta_c - \Delta_d \pm \sqrt{\Delta_d^2 + 4\Omega_d^2}\right)/2$. Hence the gap positions can be tuned by changing $\Delta_\pm$. In the following, we keep the SW on resonance, i.e. $\Delta_c=0$, and tune the PBGs structures via the changing parameters of the control field, including Rabi frequency Ω_d and detuning Δ_d.

When increasing the value of Ω_d, $|\Delta_\pm|$ increase consequently. Therefore the double PBGs move oppositely to large detunings with the widths and reflectivities being almost unchanged, and moreover, the transmissivity of the left (right) transmission region becomes low (high) due to the increase (decrease) of the probe absorption in the corresponding EIT window, as shown in Fig. 4.

As Δ_d increase from zero to the large positive detuning, the right PBG shifts to zero from the positive detuning with broadened width,

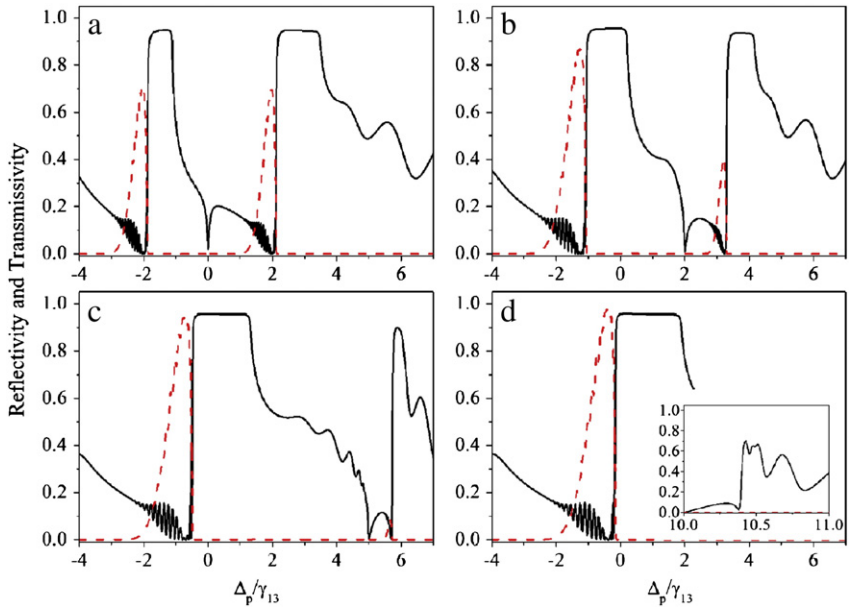

Fig. 6. Photonic band gap structure for different negative control detunings, (a) $\Delta_d=0$, (b) $\Delta_d=-2.0\gamma_{31}$, (c) $\Delta_d=-5.0\gamma_{31}$, and (d) $\Delta_d=-10.0\gamma_{31}$. Other parameters are the same as in Fig. 2. The black solid line and red dashed line correspond to the reflectivity and transmissivity, respectively.

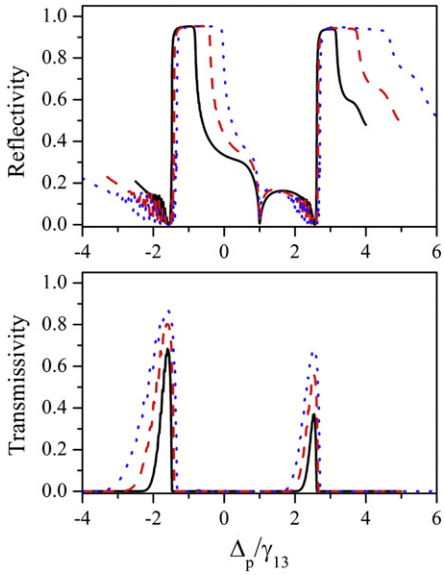

Fig. 7. Photonic band gap structure for different intensities of the standing-wave with $\Omega_0 = 15\gamma_{31}$ (black solid), $\Omega_0 = 20\gamma_{31}$ (red dashed), and $\Omega_0 = 25\gamma_{31}$ (blue dotted). Other parameters are the same as in Fig. 2.

while the left PBG becomes far away to the negative detuning with a narrowed width and then vanishes when Δ_d is large enough, as shown in Fig. 5. By numerical analysis, one obtains that $\Delta_+ = 0$ and $\Delta_- = -\infty$ in the limit of $\Delta_d \to +\infty$, and moreover, the right (left) EIT window gets wider (narrower). Finally, the double-dark resonance system turns into a Λ-configuration with a single resonance for a large Δ_d as if there is no interaction of Ω_d, hence double PBGs turn to a single one. These lead to the above evolution of the PBGs structure. Furthermore, the transmissivity is enhanced (reduced) as a result of the broadening (narrowing) of the EIT window.

If Δ_d is decreased from zero to the negative detuning, as Fig. 6 shows, the edges and widths of the double PBGs, and the transmitivity of the two transmission regions vary contrary to the case shown in Fig. 5.

Though the Rabi frequency of the coupling field Ω_0 plays no role in tuning the positions of PBGs, it can affect the gap widths. It is obvious that a large value of Ω_0 correspond to the wide EIT windows at the nodes of the SW. Therefore, both of the double PBGs can be broadened by increasing Ω_0, and the corresponding transmissivity is enhanced (see Fig. 7).

3.3. Control of light–pulse propagation

As we know, the PBG in the complex photonic structures has the ability to manipulate the flow of light. Then we concentrate on the all-optical control of the light–pulse propagation via the coherently induced double PBGs. Fig. 8 shows the reflected and transmitted intensities of an incident probe pulse impinging upon a double PBGs structure in Fig. 6(a). When most of the frequency components are inside the transmission regions, the probe pulse propagates through the atoms in the form of slow light with a large time delay, and the loss and broadening for the probe is due to the narrow transmission

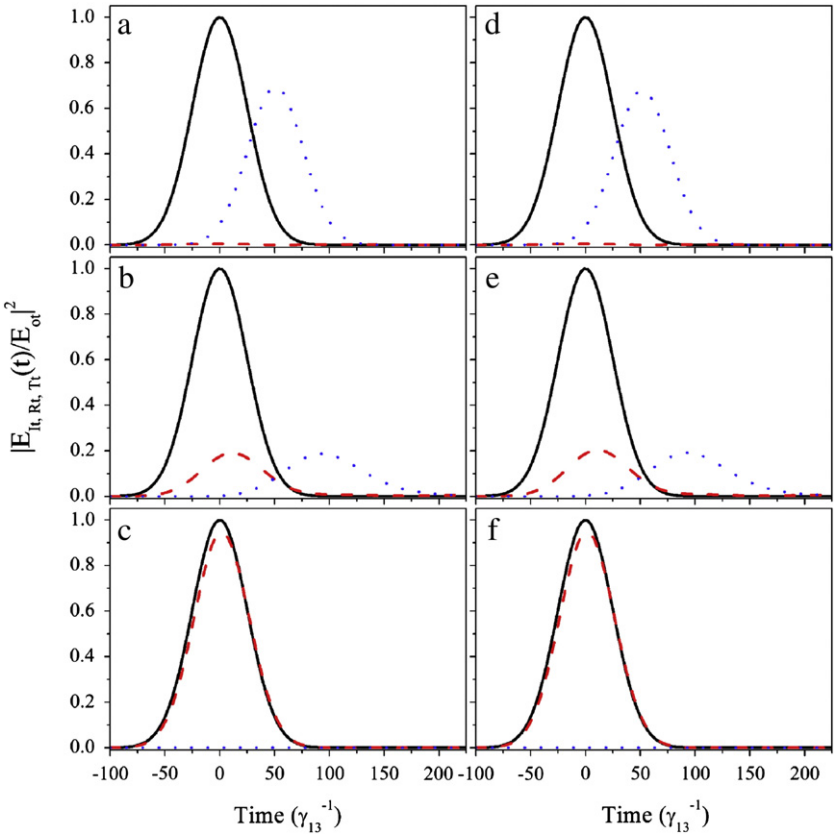

Fig. 8. Pulse dynamics of an incident (black–solid) probe impinging upon a 1.0 cm long sample with the photonic band gap structure shown in Fig. 4(a). The frequency widths and centers of the incident pulsed are $\delta_p = 0.04\gamma_{31}$, and (a) $\Delta_{p0} = -2.05\gamma_{31}$, (b) $\Delta_{p0} = -1.9\gamma_{31}$, (c) $\Delta_{p0} = -1.5\gamma_{31}$, (d) $\Delta_{p0} = 1.95\gamma_{31}$, (e) $\Delta_{p0} = 2.1\gamma_{31}$, and (f) $\Delta_{p0} = 2.5\gamma_{31}$. The reflected (red dashed) and transmitted (blue dotted) intensities are scaled to the peak intensity of the incident probe pulse.

and group-velocity dispersion in the EIT windows (Fig. 8(a),(d)). If the center frequency of the probe lies near the band edge, i.e. only the partial frequency components fall into the PBGs, the pulse splits into two, one of which is reflected and the other is transmitted. Both are broadened as a result of the decrease of the frequency components, and moreover, the latter *experiences* subluminal propagation owing to EIT (Fig. 8(b),(e)). While all frequency components of the probe move into the PBGs, the pulse is reflected with little attenuation or distortion (Fig. 8(c),(f)).

4. Conclusion

In summary, by numerical calculations and qualitative analyses, we have investigated the optical response of an SW dressed double-dark-resonance atomic system. Owing to the periodically modulated refractive index induced by the intensity pattern of the SW, double fully developed PBGs open up within the two EIT windows. The dynamically induced PBGs structure, i.e. the widths and positions, can be controlled via tuning the Rabi frequency of the SW and the transparency points which depend on the control field. Furthermore, the double PBGs scheme is more appealing than the single PBG scheme in real applications, because it allows the synchronous manipulation of the propagation for two weak light pulses with distinct frequencies. Such a scheme provides an avenue to devise novel photonic devices, e.g. double-channel all-optical routing and switching, in optical network and information processing. The double PBGs may also be exploited to achieve the deterministic quantum logic [24] and the enhancement of nonlinear interactions between light pulses [25].

Acknowledgements

This work is supported by NSFC (Grant Nos. 10774059, 11074097, 10904048, 11004079), the National Basic Research Program (Grant Nos. 2006CB921103, 2011CB921603) of the People's Republic of China, and the Graduate Innovation Fund of Jilin University.

References

[1] M. Fleischhauer, A. Imamoğlu, J.P. Marangos, Rev. Mod. Phys. 77 (2005) 633.
[2] S.E. Harris, Phys. Today 50 (1997) 36.
[3] L.V. Hau, S.E. Harris, Z. Dutton, C.H. Behroozi, Nature (London) 397 (1999) 594.
[4] M. Fleischhauer, M.D. Lukin, Phys. Rev. Lett. 84 (2000) 5094.
[5] S.E. Harris, L.V. Hau, Phys. Rev. Lett. 82 (1999) 4611.
[6] H.Y. Ling, Y.Q. Li, M. Xiao, Phys. Rev. A 57 (1998) 1338.
[7] M. Bajcsy, A.S. Zibrov, M.D. Lukin, Nature (London) 426 (2003) 638.
[8] K.R. Hansen, K. Mølmer, Phys. Rev. A 75 (2007) 053802.
[9] Y.W. Lin, W.T. Liao, T. Peters, H.C. Chou, J.S. Wang, H.W. Cho, P.C. Kuan, I.A. Yu, Phys. Rev. Lett. 102 (2009) 213601.
[10] G. Nikoghosyan, M. Fleischhauer, Phys. Rev. A 80 (2009) 013818.
[11] A. André, M.D. Lukin, Phys. Rev. Lett. 89 (2002) 143602.
[12] X.M. Su, B.S. Ham, Phys. Rev. A 71 (2005) 013821.
[13] M. Artoni, G.C. La Rocca, Phys. Rev. Lett. 96 (2006) 073905.
[14] Q.Y. He, J.H. Wu, T.J. Wang, J.Y. Gao, Phys. Rev. A 73 (2006) 053813.
[15] J.H. Wu, G.C. La Rocca, M. Artoni, Phys. Rev. B 77 (2008) 113106.
[16] J.H. Wu, M. Artoni, G.C. La Rocca, Phys. Rev. Lett. 103 (2009) 133601.
[17] J.W. Gao, J.H. Wu, N. Ba, C.L. Cui, X.X. Tian, Phys. Rev. A 81 (2010) 013804.
[18] J.W. Gao, Y. Zhang, N. Ba, C.L. Cui, J.H. Wu, Opt. Lett. 35 (2010) 709.
[19] C.L. Cui, J.H. Wu, J.W. Gao, Y. Zhang, N. Ba, Opt. Express 18 (2010) 4538.
[20] S.Q. Kuang, R.G. Wan, J. Kou, Y. Jiang, J.Y. Gao, J. Opt. Soc. Am. B 27 (2010) 1518.
[21] R.G. Wan, J. Kou, S.Q. Kuang, L. Jiang, J.Y. Gao, Opt. Express 18 (2010) 15591.
[22] M.D. Lukin, S.F. Yelin, M. Fleischhauer, M.O. Scully, Phys. Rev. A 60 (1999) 3225.
[23] C.W. Hoyt, Z.W. Barber, C.W. Oates, T.M. Fortier, S.A. Diddams, L. Hollberg, Phys. Rev. Lett. 95 (2005) 083003.
[24] I. Friedler, G. Kurizki, Phys. Rev. A 71 (2005) 023803.
[25] A. André, M. Bajcsy, A.S. Zibrov, M.D. Lukin, Phys. Rev. Lett. 94 (2005) 063902.